Specific contact resistivity of n-type Si and Ge M-S and M-I-S contacts

Jiseok Kim*, Phillip J. Oldiges‡, Hui-feng Li†, Hiroaki Niimi*, Mark Raymond*, Peter Zeitzoff*, Vimal Kamineni*, Praneet Adusumilli§, Chengyu Niu¶, and Fadoua Chafik¶
*GLOBALFOUNDRIES, Albany, NY 12203, USA, jiseok.kim@globalfoundries.com
†College of Nanoscale Science and Engineering, SUNY Polytechnic Institute, Albany, NY 12203, USA
‡International Business Machines, Hopewell Junction, NY 12533, USA
§International Business Machines, Albany, NY 12203, USA
¶STMicroelectronics, Albany, NY 12203, USA

***Abstract*—We have theoretically investigated the specific contact resistivity of n-type Si and Ge metal-insulator-semiconductor contacts with various insulating oxides. We have found a significant reduction of the contact resistivity for both Si and Ge with an insertion of insulators at low and moderate donor doping levels. However, at the higher doping levels (>10^{20} cm^{-3}), the reduction of the contact resistivity is negligible and the contact resistivity increases as the insulator thickness increaes. Thus, we have shown that the lowest possible contact resistivity can be achieved with the metal-semiconductor contact with highest possible activated doping density.**

I. Introduction

As the semiconductor devices scale down to nanometer regime, the contact resistance becomes dominant component of parasitic resistance of the devices. Thus, it is urgently required to reduce the contact resistance to meet the performace target of the future 7nm and beyond technology nodes. According to the ITRS roadmap [1], the maximum specific contact resistivity ρ_c is required to be 1.5×10^{-9} Ω.cm^2 by 2028 to meet the overall parasitic resistance requirement in the silicon (Si) MOSFET devices. In a theoretical study on the intrinsic limit of the contact resistivity within the ballistic trasport limit, it has been shown that the ITRS target is indeed possible from a theoretical perspective in a moderate doping density range for Si [2]. Yet, the lowest specific contact resistivity reported in an experiment so far for the p-type metal-semiconductor (M-S) contact (Pt-Si) is $\rho_c = 1.9\times10^{-9}$ Ω.cm^2 [3]. In order to further reduce the contact resistivity, metal-insulator-semiconductor (M-I-S) contacts have been proposed and demonstrated to depin the metal Fermi-level by inserting an ultrathin insulating layer in between metal and semiconductor leading to a reduced Schottky barrier height so the lower the contact resistivity [4]–[7]. The Schottky barrier height reduction by the Fermi level depinning effect has been theoretically investigated within the metal induced gap states (MIGS) theory [8]–[10] which has been extensively adopted in the M-I-S contact resistivity modeling to seek an optimized insulator thickness for the lowest possible contact resistivity [11], [12].
In this study, we have employed MIGS modeling [13] to describe the Fermi-level depinning due to an ultrathin insulator in between the metal and semiconductor layers. We also have employed a tunnleling model based on the transfer matrix method (TMM) to calculate the tunneling current across the given potential barrier profile. Then we have evaluated the contact resistivity as a function of doping density and insulator layer thickness for a given M-I-S contact.

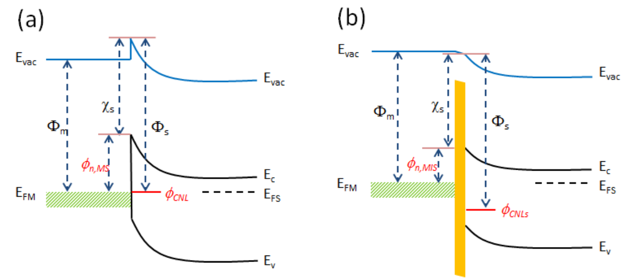

Fig. 1. Band diagram of (a) M-S and (b) M-I-S contact where the metal workfunction, electron affinity, charge neutrality level, Schottky barrier height, Fermi level, vacuum level, conduction and valence band edge of the semiconductor are denoted as Φ_m, χ_s, ϕ_{CNL}, ϕ_n, E$_{FM}$(E$_{FS}$), E$_{vac}$, E$_c$ and E$_v$, respectively.

II. Methodology

Figure 1 (a) shows the schematic band diagram of the Schottky barrier for the M-S contact where the one-dimensional (1D) non-selfconsistent potential barrier profile can be written as [14],

$$V(z) = \frac{q^2 N_D}{2\epsilon_s}(W_D - z)^2 - \frac{q^2}{16\pi\epsilon_s z}\ , \tag{1}$$

where the N_D is the doping density in the semiconductor, permittivity of the semiconductor ϵ_s=11.7ϵ_0, and the depletion width $W_D = \sqrt{2\epsilon_s(V_{bi} - V)/qN_D}$. V is the applided bias volage to the contact and the surface potential is $qV_{bi} = \phi_n - (E_c - E_{FS})$ where the position of the conduction band relative to the Fermi-level is approximated as [15],

$$\frac{E_c - E_{FS}}{k_B T} = \frac{\ln\gamma}{1-\gamma} + \left(\frac{3\sqrt{\pi}\gamma}{4}\right)^{2/3} + \frac{8\sqrt{\pi}\gamma}{3(4+\sqrt{pi}\gamma)^2}\ , \tag{2}$$

where k_BT=0.0258 eV at T=300 K and the $\gamma = N_D/N_c$. The effective density of states for electrons is $N_c = 2(2\pi m^*_{dc} k_B T/h^2)^{3/2}$ where the density of states effective mass m^*_{dc} for electrons is 1.09 m_e and 0.56 m_e for Si and Ge, respectively. Note that the metal Fermi-level E_{FM} is aligned to the charge neutrality level (ϕ_{CNL}) (measured from the valence

978-1-4673-7860-4/15/$31.00 ©2015 IEEE

TABLE I. MATERIAL PARAMETERS FOR SEMICONDUCTORS

	E_g(eV)	$\epsilon(\epsilon_0)$	S	χ(eV)	ϕ_{CNL}(eV)	α(Å)	δ_s(Å)
Si	1.12	11.7	0.296	4.05	0.35	2.35	3.0
Ge	0.66	16	0.217	4.13	0.11	2.45	4.0

TABLE II. METAL WORKFUNTIONS

	Pt	Ti	Cu	Al	Ag	Au	Ni
Φ_m(eV)	5.12	4.33	4.53	4.1	4.26	5.1	5.04

TABLE III. MATERIAL PARAMETERS FOR INSULATORS

	$\epsilon(\epsilon_0)$	$\epsilon_\infty(\epsilon_0)$	E_g(eV)	χ(eV)	ϕ_{CNL}(eV)	a_0(Å)	m^* (m_0)
HfO_2	25.0	4.0	6.0	2.4	3.7	5.08	0.17
La_2O_3	30.0	4.0	6.0	2.0	2.4	3.94	0.26
Al_2O_3	9.0	3.4	8.8	1.0	5.5	4.79	0.2
TiO_2	80.0	7.8	3.05	3.9	2.2	4.59	0.3
Si_3Ni_4	7.5	3.8	5.3	2.1	2.6	7.61	0.2
GeO_2	5.9	1.8	4.3	2.24	3.34	4.4	0.7
ZnO	9.0	3.7	3.4	4.6	3.1	3.25	0.3

band maximum) of the Si due to the MIGS density near the interface leading to the Fermi-level pinning. Thus the Schottky barrier height is determined by the Fermi-level pinning factor S [10], [16] and the Φ_S which is measured from the vacuum to the ϕ_{CNL},

$$\phi_n = S(\Phi_m - \Phi_S) + (\Phi_S - \chi_s) \ . \quad (3)$$

The pinning factor S is related to the MIGS density as following [17],

$$S = \frac{1}{1 + (q^2 D_{MIGS,0}\delta_s)/(\epsilon_s)} \ , \quad (4)$$

where the $D_{MIGS,0} = 1/(\pi\alpha^2 E_g)$ is the MIGS density at zero insulator thickness in between the metal and semiconductor contact. α is the atomic bonding length, δ_s is the MIGS decay length [9] and the E_g is the band gap of the semicoductor. We have used material parameters for semiconductors and metal workfunctions as shown in Table I and II and the calculated pinning factor S is shown in Table I.

With an insertion of an insulator layer in between the metal and semiconductor contact as shown in Fig. 1 (b), we can re-write the Eq. 3 as,

$$\phi_n = \Phi_S - \chi_s - \psi_s \ , \quad (5)$$

where the equilibrium surface potential corresponding to the total band bending within the semiconductor [13],

$$\psi_s(C_s) = -\frac{C_I}{C_I + C_S}\Phi_{MS} - \frac{C_{iI}}{C_{iI} + C_{iS}}\Delta_{IS} \ , \quad (6)$$

where the C_I and C_S are the surface capacitance densities for the insulator and semiconductor, respectively, while C_{iI} and C_{iS} are insulator-semiconductor dipole capacitance densities for the insulator and semiconductor, respectively. Δ_{IS} is the insulator-semiconductor dipole voltage,

$$\Delta_{IS} = (1 - S_{IS})[\phi_{CNL,s} - \phi_{CNL,I}] \ , \quad (7)$$

where the S_{IS} is the pinning factor for the insulator-semiconductor interface and the $\phi_{CNL,I}$ is the charge neutrality level of the insulator as listed in Table. III for various insulators. In order to evaluate the n-type SBH in Eq. 5, the surface potential ψ_s should be assessed simultaneously which is described in more detail in Refs. [12], [13], [18]. Note the Φ_{MS} in Eq. 6 is,

$$\Phi_{MS} = \Phi_{M,eff} - \Phi_S \ , \quad (8)$$

where the effective metal workfuction $\Phi_{M,eff}$ is given as,

$$\Phi_{M,eff} = S(t_{ox})\Phi_M + [1 - S(t_{ox})]S(t_{ox})\Phi_S \ , \quad (9)$$

in terms of the insulator thickness dependent pinning factor,

$$S(t_{ox}) = \left(1 + q^2\frac{D_{MIGS}(t_{ox})(\delta_s\epsilon_{ox} + t_{ox}\epsilon_s)}{\epsilon_{ox}\epsilon_s}\right)^{-1} \ , \quad (10)$$

where the t_{ox} is the insulator thickness and ϵ_{ox} is the dielectric constant of the insulator. Also,the insulator thickness dependent MIGS density can be written as,

$$D_{MIGS}(t_{ox}) = D_{MIGS,0}\exp[-t_{ox}/\delta_{ox}] \ , \quad (11)$$

where $\delta_{ox} = 2\hbar^2\pi/(m_e a_{0,ox}E_{g,ox})$ where the $a_{0,ox}$ and $E_{g,ox}$ are the lattice constant and band gap of the insulator, respectively [17]. Note the Eqs. 5, 10 and 11 consistently converge to the Eqs. 3 and 4 without the insulator layer (i.e. $t_{ox} \to 0$).

Once we have established 1D homogeneous Schottky barrier profile with and without an insulator layer using the MIGS theory, we then have calculated the net current density using the Tsu-Esaki formula within parabolic band and effective mass approximation [19],

$$J = \sum_{i=1}^{nvalley}\frac{qm_{c,i}^* k_B T}{2\pi^2\hbar^3}\int_{E_{min}}^{\infty} dE_z T_i(E_z)\ln\left\{\frac{1 + e^{(E_{FM}-E_z)/k_BT}}{1 + e^{(E_{FS}-E_z)/k_BT}}\right\} , \quad (12)$$

where $m_{c,i}^*$ is the orientation dependent conductivity effective mass at each equi-energy surface (represented by index i and the number of equi-energy surface '$nvalley$' is six and four at the conduction band minimum of Si and Ge, respectively) [20]. We have taken into account the multi-valley tunneling by summing up the current density at all conduction band valleys. The tunneling probability $T_i(E_z)$ at a given incident electron energy E_z at each conduction band valley i is evaluated using the conventional transfer matrix method (TMM) [21] with a boundary condition used in Ref. [22],

$$T_i(E_z) = \frac{m_{tun,N+1}^{i*}}{m_{tun,0}^{i*}}\frac{k_{N+1}}{k_0}\left|\frac{k_0}{k_{N+1}}\right|^2\left|\frac{1}{M_{22}}\right|^2 \quad (13)$$

where the indices 0 and $N+1$ represent the first (in the metal) and last (in the semiconductor) discretized grid points across the potential barrier profile, M_{22} is the matrix element of the transfer matrix and the wavevector $k_{N+1} = \sqrt{2m_{tun,N+1}^{i*}(E_z - V_{N+1})}/\hbar$. Note that we have used the orientation depedent tunneling effective mass m_{tun}^{i*} at each conduction band valley i [23] when evaluating the tunneling probability. Finally, the specific contact resistivity $\rho_c = dV/dJ$ is then numerically evaluated at a very small applied voltage $V = 10^{-5}$ V at which the ρ_c converges by varying V.

III. RESULTS AND DISCUSSIONS

Figure 2 (a) shows the ρ_c for the n-type M-S contact for (001) Si at a given Schottky barrier height varying from 0.2 eV to 0.8 eV as a function of donor doping density at T=300 K. As expected the ρ_c is smaller at lower barrier height and continuously decreases as the doping density increases. In addition, the barrier height dependence on the ρ_c becomes

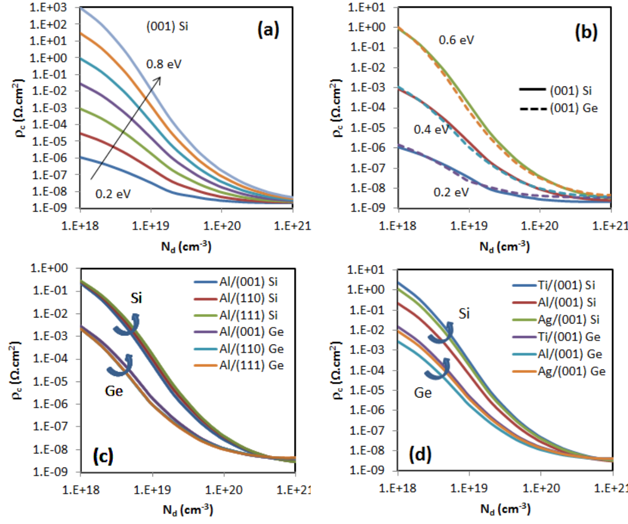

Fig. 2. Contact resistivity of M-S contact as a function of doping density for (a) (001) Si at a given Schottky barrier height, (b) (001) Si and Ge at the barrier height 0.2, 0.4 and 0.6 eV, (c) (001), (110) and (111) Si and Ge with Al metal contact, and (d) (001) Si and Ge with Ti, Al, and Ag metal contacts.

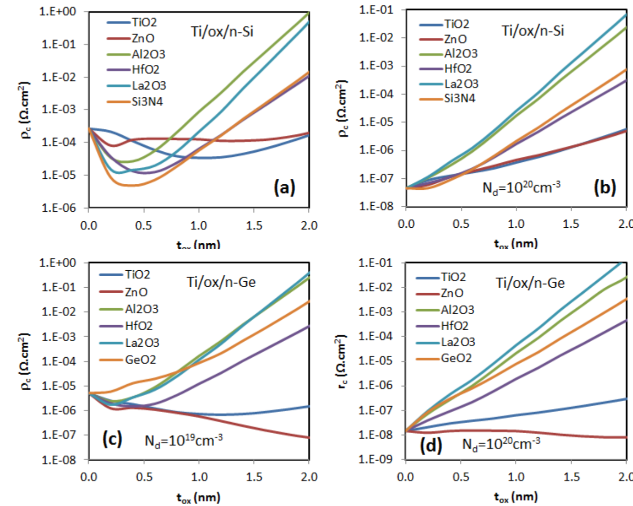

Fig. 3. Contact resistivity of M-I-S contact as a function of insulator thickness for Ti/ox/n-Si at (a) N_d=10^{19} cm^{-3} and (b) N_d=10^{20} cm^{-3}, and Ti/ox/n-Ge at (c) N_d=10^{19} cm^{-3} and (d) N_d=10^{20} cm^{-3}.

negligible at ultra high doping region ($N_d > 10^{21}$ cm^{-3}) and the ρ_c converges to $\sim 2.1\times10^{-9}$ and begins to increase with even higher doping which is due to the interplay between the matrix element M_{22} and the wavevector k_{N+1}. Because the wavevector k_{N+1} in Eq. 13 becomes dominant at very high dopings as the Fermi-level deeply penetrates into the conduction bands while the matrix element M_{22} converges to unity. Thus the tunneling probability is reduced which leads to the decreased tunneling current.

Figure 2 (b) shows that there is only slight differences in ρ_c between Si and Ge at a given barrier height and at a given crystal orientation. Also, a slight orientation dependence can be seen in Fig. 2 (c) (lower ρ_c with (001) orentation for Si while lower

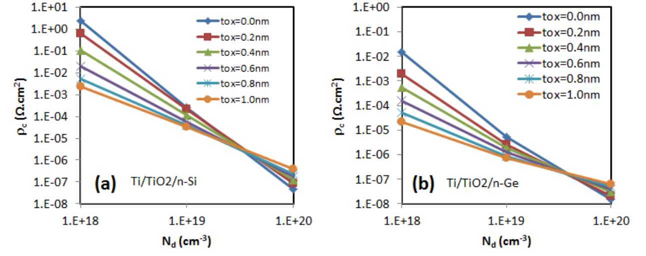

Fig. 4. Contact resistivity of M-I-S contact as a function of doping density for (a) Ti/TiO_2/n-Si and for (b) Ti/TiO_2/n-Ge at a given TiO_2 thickness

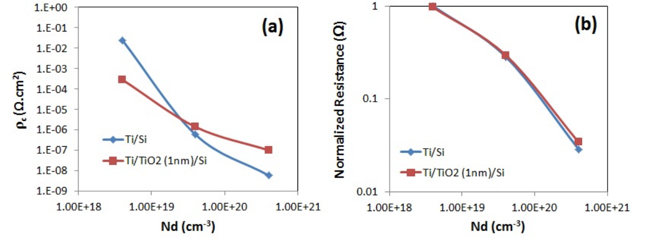

Fig. 5. Contact resistivity from the calculation for (a) and normalized contact resistance from the measurement for (b) of Ti/n-Si and Ti/TiO_2 (1nm)/n-Si contact as a function of doping density

ρ_c with (111) orientation for Ge than other crystal orientations in this study) due to mainly orientation dependent coductivity and tunneling effective masses for electrons. Figure 2 (d) shows the metal workfunction (Φ_M) dependence on the ρ_c for (001) Si and Ge and it is shown that the Al (Φ_M=4.1 eV) gives lower ρ_c than any other metals used in this study (Pt, Ti, Cu, Ag, Au, and Ni) because of the lower Schottky barrier height with Al (0.56 eV for Si and 0.427 eV for Ge) which gives ρ_c=3.04×10^{-9} Ω.cm^2 for Si and ρ_c=4.02×10^{-9} Ω.cm^2 for Ge at N_D=10^{21} cm^{-3}. Though we have to reiterate that the there is no sigficant difference in ρ_c at ultra high activation doping concentrations no matter what metal workfunction, crystal orientation and even semiconductors are used. Therefore, it is critically required to maximize the activated doping level in the source and drain contact region for the lowest possible contact resistivity.

Having discussed the ρ_c for the M-S contact, we have shown the ρ_c as a function of insulator thickness (t_{ox}) for M-I-S contact in Fig. 3 with various insulators (HfO_2, La_2O_3, Al_2O_3, TiO_2, Si_3N_4, GeO_2, ZnO) for Si and Ge with Ti as a contact metal. As clearly seen in Fig. 3 (a) and (c), the ρ_c can be significantly reduced (up to two orders of magnitude) by an insertion of insulating layers for both Si and Ge at moderate doping level N_D=10^{19} cm^{-3} due to the Fermi-level depinning effect leading to reduced Schottky barrier height [7], [12], [18]. However, the ρ_c begins to increase when the thickness of the insulator becomes thicker than their optimized thicknesses as the barrier tunneling through the insulator offsets the ρ_c benefit from the reduced barrier height. We have found that the the lowest ρ_c can be achieved with Si_3N_4 for Si and ZnO for Ge with optimized insulator thicknesses t_{ox} $\sim$0.5 nm and $t_{ox}$$\sim$3.0 nm, respectively, at the moderate doping density. However, there is no (or negligible) reduction of the ρ_c by the insulator at high doping density N_D=10^{20} cm^{-3} as shown in Fig. 3 (b) and (d) because the ρ_c benefit from the reduced

barrier height becomes negligible at high doping density as already shown in Fig. 2. It is worth to note that the ρ_c at the high doping N_D=10^{20} cm^{-3} without the insulator ($i.e.$ M-S contact) is still lower than the ρ_c at the moderate doping N_D=10^{19} cm^{-3} with optimized insulator thickness. Therefore we can conclude that there is no benefit (or at least questionable benefit) for the lowest possible ρ_c by employing the M-I-S contact with ultra high doping density.

One can see more clearly in Fig. 4 that the lowest ρ_c for both Si and Ge can be achieved at N_D=10^{20} (or higher doping density) with M-S contact as opposed to the previous theoretical calculations [12], [18]. The same trend has been also confirmed by our experiment on the contact resistance of Ti/TiO_2 (1nm)/Si contact as shown in Fig. 5 (b) in which slightly lower contact resistance was observed from the M-S contact at higher doping level N_D=4×10^{20} cm^{-3}. However, the improvement (or degradation) of the resistance at high (or lower) doping level is not as significant as the calculated ρ_c as shown in Fig. 5 (a) in which the ρ_c improvement (or degradation) is about 10 times (or 100 times) at high (or lower) doping density from the M-S contact when compared the M-I-S contact. We believe that the small improvement of the resistance from the experiment at high doping is due to the existence of the native oxides as well as the poor quality of the interface formation.

IV. Conclusion

We have theoretically calculated the contact resistivity for M-S and M-I-S contacts with various insulators. We have employed MIGS modeling to describe the Fermi-level depinning effect by an insertion of the insulator in between the metal and semiconductor contact. Also, we have calculated the current density across the Schottky barrier profile within the parabolic and effective mass approximation by considering multi-valley and orientation dependent effective masses. We have shown that it is critically required to maximize the activated doping density in the M-S contact to achieve the lowest possible contact reistivity regardless of the crystal orientation, metal and semiconductor. In addition, we have also shown that the lowest contact resistivity can be achieved with M-S contact with ultra high doping density rather than M-I-S which is consistently observed from our experiment on contact resistance in Ti/TiO_2/Si contact.

Acknowledgment

This work was performed by the Research and Development Alliance Teams at various IBM Research Development Facilities. The authors also would like to thank to Prof. John F. Wager at Oregon State University, Prof. Massimo V. Fischetti at the University of Texas at Dallas, Dr. Crystal Kenney and Dr. Sudarshan Narayanan at Globalfoundries for their vauable discussions.

References

[1] "International technology roadmap for semiconductors," 2013. [Online]. Available: http://www.itrs.net

[2] J. Maassen, C. Jeong, A. Baraskar, M. Rodwell, and M. Lundstrom, "Full band calculations of the intrinsic lower limit of contact resistivity," *Applied Physics Letters*, vol. 102, no. 11, pp. 111 605–111 605, 2013.

[3] N. Stavitski, M. Van Dal, A. Lauwers, C. Vrancken, A. Kovalgin, and R. Wolters, "Systematic tlm measurements of nisi and ptsi specific contact resistance to n-and p-type si in a broad doping range," *Electron Device Letters, IEEE*, vol. 29, no. 4, pp. 378–381, 2008.

[4] D. Connelly, C. Faulkner, P. Clifton, and D. Grupp, "Fermi-level depinning for low-barrier schottky source/drain transistors," *Applied physics letters*, vol. 88, no. 1, p. 012105, 2006.

[5] M. Kobayashi, A. Kinoshita, K. Saraswat, H.-S. P. Wong, and Y. Nishi, "Fermi level depinning in metal/ge schottky junction for metal source/drain ge metal-oxide-semiconductor field-effect-transistor application," *Journal of applied physics*, vol. 105, no. 2, p. 023702, 2009.

[6] M.-H. Liao and L. Chang, "Experimental demonstration for the implant-free in0. 53ga0. 47as quantum-well metal-insulator-semiconductor field-effect transistors with ultra-low source/drain resistance," *Applied Physics Letters*, vol. 103, no. 7, p. 072102, 2013.

[7] J.-Y. Lin, A. M. Roy, and K. C. Saraswat, "Reduction in specific contact resistivity to ge using interfacial layer," *Electron Device Letters, IEEE*, vol. 33, no. 11, pp. 1541–1543, 2012.

[8] W. Mönch, "Barrier heights of real schottky contacts explained by metal-induced gap states and lateral inhomogeneities," *Journal of Vacuum Science & Technology B*, vol. 17, no. 4, pp. 1867–1876, 1999.

[9] J. Tersoff, "Schottky barrier heights and the continuum of gap states," *Physical Review Letters*, vol. 52, no. 6, p. 465, 1984.

[10] W. Mönch, "Electronic properties of ideal and interface-modified metal-semiconductor interfaces," *Journal of Vacuum Science & Technology B*, vol. 14, no. 4, pp. 2985–2993, 1996.

[11] A. Agrawal, N. Shukla, K. Ahmed, and S. Datta, "A unified model for insulator selection to form ultra-low resistivity metal-insulator-semiconductor contacts to n-si, n-ge, and n-ingaas," *Applied Physics Letters*, vol. 101, no. 4, p. 042108, 2012.

[12] S. Gupta, P. P. Manik, R. K. Mishra, A. Nainani, M. C. Abraham, and S. Lodha, "Contact resistivity reduction through interfacial layer doping in metal-interfacial layer-semiconductor contacts," *Journal of Applied Physics*, vol. 113, no. 23, p. 234505, 2013.

[13] J. F. Wager and J. Robertson, "Metal-induced gap states modeling of metal-ge contacts with and without a silicon nitride ultrathin interfacial layer," *Journal of Applied Physics*, vol. 109, no. 9, p. 094501, 2011.

[14] M. Furno, F. Bonani, and G. Ghione, "Transfer matrix method modelling of inhomogeneous schottky barrier diodes on silicon carbide," *Solid-state electronics*, vol. 51, no. 3, pp. 466–474, 2007.

[15] N. Nilsson, "An accurate approximation of the generalized einstein relation for degenerate semiconductors," *physica status solidi (a)*, vol. 19, no. 1, pp. K75–K78, 1973.

[16] J. Robertson, "Band offsets of wide-band-gap oxides and implications for future electronic devices," *Journal of Vacuum Science & Technology B*, vol. 18, no. 3, pp. 1785–1791, 2000.

[17] W. Monch, "On the physics of metal-semiconductor interfaces," *Reports on Progress in Physics*, vol. 53, no. 3, p. 221, 1990.

[18] A. Agrawal, N. Shukla, K. Ahmed, and S. Datta, "A unified model for insulator selection to form ultra-low resistivity metal-insulator-semiconductor contacts to n-si, n-ge, and n-ingaas," *Appl. Phys. Lett.*, vol. 101, no. 4, p. 042108, 2012.

[19] R. Tsu and L. Esaki, "Tunneling in a finite superlattice," *Applied Physics Letters*, vol. 22, no. 11, pp. 562–564, 1973.

[20] K. K. Ng and R. Liu, "On the calculation of specific contact resistivity on¡ 100¿ si," *Electron Devices, IEEE Transactions on*, vol. 37, no. 6, pp. 1535–1537, 1990.

[21] Y. Ando and T. Itoh, "Calculation of transmission tunneling current across arbitrary potential barriers," *Journal of applied physics*, vol. 61, no. 4, pp. 1497–1502, 1987.

[22] W. A. Harrison, A. Goebel, and P. A. Clifton, "Effective-mass theory of metal-semiconductor contact resistivity," *Applied Physics Letters*, vol. 103, no. 8, p. 081605, 2013.

[23] C. Crowell, "Richardson constant and tunneling effective mass for thermionic and thermionic-field emission in schottky barrier diodes," *Solid-State Electronics*, vol. 12, no. 1, pp. 55–59, 1969.